

## Chemical Composition of Celandine (*Chelidonium majus* L.) Extract and its Effects on *Botrytis tulipae* (Lib.) Lind Fungus and the Tulip

Marcel PARVU<sup>1\*</sup>, Laurian VLASE<sup>2</sup>, Laszlo FODORPATAKI<sup>3</sup>, Ovidiu PARVU<sup>4</sup>, Oana ROSCASCASIAN<sup>5</sup>, Csaba BARTHA<sup>3</sup>, Lucian BARBU-TUDORAN<sup>6</sup>, Alina Elena PARVU<sup>7</sup>

<sup>1</sup>Babes-Bolyai University, Faculty of Biology and Geology, Department of Biology, 42 Republicii St, 400015 Cluj-Napoca, Romania; [marcel.parvu@ubbcluj.ro](mailto:marcel.parvu@ubbcluj.ro) (\*corresponding author)

<sup>2</sup>Iuliu Hatieganu University of Medicine and Pharmacy, Faculty of Pharmacy, Department of Pharmaceutical Technology and Biopharmaceutics, 12 Ion Creanga St, 400010 Cluj-Napoca, Romania; [laurian.vlase@yahoo.com](mailto:laurian.vlase@yahoo.com)

<sup>3</sup>Babes-Bolyai University, Hungarian Department of Biology and Ecology, 1 Mihail Kogalniceanu St, 400084 Cluj-Napoca, Romania; [lfodorp@gmail.com](mailto:lfodorp@gmail.com); [barthacsabi@gmail.com](mailto:barthacsabi@gmail.com)

<sup>4</sup>Babes-Bolyai University, Faculty of Mathematics and Computer Science, 1 Mihail Kogalniceanu St, 400084 Cluj-Napoca, Romania; [ovidiu.parvu@gmail.com](mailto:ovidiu.parvu@gmail.com)

<sup>5</sup>Babes-Bolyai University, A. Borza Botanical Garden, 42 Republicii St, 400015 Cluj-Napoca, Romania; [casioana@yahoo.com](mailto:casioana@yahoo.com)

<sup>6</sup>Babes-Bolyai University, Electron Microscopy Center, 5-7 Clinicilor St, 400006 Cluj-Napoca, Romania; [lucianbarbu@yahoo.com](mailto:lucianbarbu@yahoo.com)

<sup>7</sup>Iuliu Hatieganu University of Medicine and Pharmacy, Faculty of Medicine, Department of Pathophysiology, 3 Victor Babes St, 400012 Cluj-Napoca, Romania; [parvualinaelena@yahoo.com](mailto:parvualinaelena@yahoo.com)

### Abstract

In this study, the content of chelidonine and berberine alkaloids, and sterols and phenols in the *Chelidonium majus* plant extract were analyzed. Subsequently, the effects of the extract on the germination and growth of *Botrytis tulipae* fungus on nutritive medium were compared to the effects of fluconazole. The plant extract was used at the minimum inhibitory concentration on *B. tulipae* developed in tulip leaves and the *in vivo* effects were investigated. The influence of different concentrations of *C. majus* extract on the physiological processes of the tulip (gas exchange parameters, photosynthetic light use efficiency, and induced chlorophyll fluorescence) were also tested to assess the applicability of the extract for the protection of ornamental plants against fungal infection. Our results demonstrated that 2% celandine extract does not significantly change the gas exchange parameters (transpiration rate, carbon dioxide uptake, and stomatal conductivity) of leaves exposed for 2 h, and does not interfere with the photochemical processes in the leaves. However, in higher concentrations, it increases the transpiration rate and net carbon dioxide influx. At concentrations of 15% and 20%, the extract lowers the potential quantum yield efficiency of photosystem II and the vitality index of the photosynthetic apparatus. Therefore we recommend the use of lower concentrations ( $\leq 6\%$ ) of celandine extract for the biological protection of tulips against gray mold.

**Keywords:** alkaloids, antifungal action, chlorophyll fluorescence, electron microscopy, leaf gas exchange, tulip fire

### Introduction

The *Botrytis* genus comprises over 20 species (Beever and Weeds, 2007), and *Botrytis* diseases are one of the most common and widely distributed; they have been identified on vegetables, ornamentals, fruits, and some field crops worldwide (Agrios, 2005). The members of this genus include *Botrytis cinerea* Pers., *Botrytis allii* Munn, *Botrytis fabae* Sardina, *Botrytis paeoniae* Oudem., and *Botrytis tulipae* (Lib.) Lind (Elad *et al.*, 2007).

*Botrytis* blight, which is also known as tulip fire, or tulip mold, is the most common and destructive disease to tulips, and is caused by the fungus *B. tulipae* (Hong *et al.*, 2002; Staats *et al.*, 2007). The fungus attacks all parts of the tulip and can rapidly kill its host's tissue and continue growing on the dead remains (Webster and Weber, 2007).

*B. tulipae* produces abundant gray mycelium and long, branched conidiophores with one-celled, ovoid conidia. The conidiophores and clusters of conidia form a grape-like cluster (Agrios, 2005; Webster and Weber, 2007).

The ability of *B. tulipae* to infect living host plants may result from a combination of at least 4 factors: (1) possession of pathogenic factors (e.g., toxins and cell-wall degrading enzymes) that confer the ability to kill and invade plant tissue; (2) the ability to avoid or counteract plant resistance mechanisms; (3) the ability to survive outside host-plant tissue under less favorable conditions (e.g., low humidity and UV irradiation); and (4) the ability to reproduce and disperse (Staats *et al.*, 2005).

Because tulips occupy an important position among flowering plants cultivated worldwide and because gray

mold is present each year in the crop, protection measures against tulip fire are vital (Agrios, 2005). The application of fungicides to control gray mold of plants is frequently used; however, the control of *Botrytis* in the field through chemical sprays is only partially successful, especially in cool, damp weather. Indeed, *Botrytis* strains resistant to several systemic fungicides, as well as some resistant to broad-spectrum fungicides have been found in various crops sprayed with these chemicals (Agrios, 2005; Webster and Weber, 2007). Plant fungicides based on synthetic chemicals cause severe and long-term environmental pollution, are highly and acutely toxic, and are carcinogenic to humans and animals (Strange and Scott, 2005). In addition, pathogens may become resistant to many of these chemicals. Consequently, the aim of new antifungal strategies is to develop drugs that combine low cost with sustainability, high efficacy, restricted toxicity, and increased safety for humans, animals, host plants and ecosystems. Biological control has become popular worldwide because fungicides of biological origin are biodegradable and have been demonstrated to be specifically effective against target organisms (Barker and Rogers, 2006; Carrillo-Munoz et al., 2006; Fatehi et al., 2005; Strange and Scott, 2005; Ienaşcu et al., 2008).

Therefore, identifying new methods to control gray mold is an important requirement, in the protection of cultivated plants. In particular, the biological control of *Botrytis* species is very important and may be done via a variety of methods, which include the use of microbial antagonists (Elad and Stewart, 2004), and plant extracts (Choi et al., 2004; Pârnu and Pârnu, 2011; Wilson et al., 1997). Plants are rich in a wide range of bioactive secondary metabolites such as tannins, terpenoids, alkaloids, and flavonoids that are reported to have *in vitro* antifungal properties. In addition, a series of molecules that possess antifungal activity against different strains of fungus have been found in plants. These molecules may be directly used or exploited as models to develop better molecules (Arif et al., 2011).

The *B. tulipae* fungus is found every year on tulips from Cluj-Napoca, Romania. We have studied the *in vitro* and *in vivo* effects of *C. majus* against gray mold on tulips because previous studies have shown that the *C. majus* extract has an antifungal effect (Matos et al., 1999; Pârnu et al., 2008) against phytopathogenic fungi. In brief, we determined the chemical composition of the *C. majus*, specifically, the content of chelidonine and berberine alkaloids, sterols, and polyphenols. In addition, the antifungal activity of *C. majus* on *B. tulipae* germination and growth was evaluated and the *in vivo* ultrastructural changes present in the tulip leaves attacked by tulip fire and treated with the *C. majus* plant extract at the minimum inhibitory concentration (MIC) for 2 h. Finally, we investigated the effects of different concentrations of *C. majus* extracts on the physiological processes of tulip plants, such as gas exchange parameters (transpiration rate, carbon dioxide uptake, and

stomatal conductance) and efficiency indicators of photosynthetic light use revealed by induced *in vivo* chlorophyll fluorescence. The main aim of this study was to introduce the *C. majus* extract to the practice of biological disease management in tulip cultures.

## Materials and methods

### *Plant material*

Celandine (*C. majus* L.) was collected from the A. Borza Botanical Garden of Cluj-Napoca (46°45'36"N and 23°35'13"E) in April 2010 and was identified by Dr. M. Parvu, Babes-Bolyai University of Cluj-Napoca. A voucher specimen (CL 663 692) is deposited at the Herbarium of Babes-Bolyai University, Cluj-Napoca, Romania.

### *Preparation of fungal colony*

*B. tulipae* (Lib.) Lind was isolated from a tulip (CL 663 693) and was identified in the Mycology Laboratory, Babes-Bolyai University, Cluj-Napoca, Romania, by Dr. M. Parvu. Colonies were obtained in Petri dishes on Czapek-agar medium (BD Difco, Budapest, Hungary), by inoculation in the central point with *B. tulipae* spore suspension ( $1 \cdot 10^5$  conidia·mL<sup>-1</sup>) and incubation at 22 °C for 5 days.

### *Preparation of alcoholic plant extract*

Fresh *C. majus* herba (leaves, stems, and flowers fragments of 0.5 – 1.0 cm) was extracted with 70% ethanol (Merck, Bucuresti, Romania) in the Mycology Laboratory of Babes-Bolyai University, Cluj-Napoca, Romania by cold repercolation method (Mishra and Verma, 2009; Sundaram and Gurumoorthi, 2012), at room temperature, for 3 days (Sundaram and Gurumoorthi, 2012). The *C. majus* extract, containing 1 g plant material in 1 mL of 35% ethanol (w/v), was obtained by filtration. From this initial solution, dilutions were made with distilled water to obtain final concentrations of 2%, 6%, 10%, 15%, and 20%.

### *Chemical composition of the C. majus extract*

#### *Determinations of chelidonine and berberine alkaloids*

A high-performance liquid chromatography method coupled with mass spectrometry (LC/MS) was accessed to quantify the amounts of berberine and chelidonine in the *C. majus* extract (Wu et al., 2005).

The LC/MS system was an Agilent 1100 Series HPLC system (Agilent Technology Co., Ltd., USA) that consisted of a binary pump, degasser, autosampler, thermostat operating at 48 °C, VL ion trap detector, and a UV detector. Chromatographic separation was performed on a Zorbax SB-C18 column (100mm · 3.0mm i.d., 3.5µm; Agilent) preceded by a 0.5 µm online filter.

The mobile phase consisted of acetonitrile and 0.1% (v/v) formic acid in water at 18:82 (v/v) and was delivered

at a flow rate of  $1 \text{ mL} \cdot \text{min}^{-1}$ . The autosampler injection volume was set at  $10 \text{ } \mu\text{L}$ . The mass spectrometer operated using an ESI source in the positive mode and was set for isolation and fragmentation of the berberine molecular ion with  $m/z = 336$  and the chelidonium ion with  $m/z = 354$ .

The quantification of berberine was based on the sum of ions with  $m/z = 291.9$  and  $321.0$  from the MS spectrum of the parent ion (Fig. 1a). Chelidonium was quantified based on the sum of the ions with  $m/z 275, 305,$  and  $323$  (Fig. 1b). The calibration curves were linear in the range of  $6.8\text{--}68 \text{ ng} \cdot \text{mL}^{-1}$  for berberine and  $14\text{--}140 \text{ ng} \cdot \text{mL}^{-1}$  for chelidonium, with a correlation coefficient greater than 0.997.

#### Identification and quantitative determinations of the polyphenols

A high-performance liquid chromatography method coupled with mass spectrometry (LC/MS) was used to analyze the polyphenolic compounds in the *C. majus* plant extract. The method used was a previously published HPLC method with minor changes (Nencu *et al.*, 2012; Compaore *et al.*, 2012; Meda *et al.*, 2011). The method is suitable for qualitative (18 compounds) and quantitative (14 compounds) analyses. In this study, 18 standards of the polyphenolic compounds were used, namely, caftaric acid, gentisic acid, caffeic acid, chlorogenic acid, paracoumaric acid, ferulic acid, sinapic acid, hyperoside, isoquercitrin, rutoside, myricetol, fisetin, quercitrin, quercetol, patuletine, luteolin, kaempferol, and apigenin.

#### Apparatus and chromatographic conditions

The experiments were performed using an Agilent 1100 HPLC Series system (Agilent) equipped with a degasser, binary gradient pump, column thermostat, autosampler, and UV detector. The HPLC system was coupled with an Agilent 1100 mass spectrometer (LC/MSD ion trap VL). For the separation, a reverse-phase analytical column was employed (Zorbax SB-C18  $100 \times 3.0 \text{ mm i.d.}, 3.5 \text{ } \mu\text{m}$  particle); the temperature was  $48 \text{ } ^\circ\text{C}$ . The compounds were detected in both the UV and MS mode. The UV detec-

tor was set at  $330 \text{ nm}$  until  $17.5 \text{ min}$ , and then at  $370 \text{ nm}$  for the remainder of the experiment. The MS system used an electrospray ion source in the negative mode. The chromatographic data were processed using ChemStation and DataAnalysis software from Agilent. The mobile phase was a binary gradient prepared from methanol and a solution of  $0.1\%$  (v/v) acetic acid. The elution started with a linear gradient, beginning with  $5\%$  methanol and ending at  $42\%$  methanol, for  $35 \text{ min}$ ; isocratic elution followed for the next  $3 \text{ min}$  with  $42\%$  methanol. The flow rate was  $1 \text{ mL} \cdot \text{min}^{-1}$  and the injection volume was  $5 \text{ } \mu\text{L}$ .

#### Polyphenols

The MS signal was used only for qualitative analysis based on the specific mass spectra of each polyphenol. The MS spectra obtained from a standard solution of polyphenols were integrated in a mass spectra library. Subsequently, the MS traces/spectra of the analyzed samples were compared to spectra from the library, which allowed the positive identification of compounds, based on spectral matches. The UV trace was used for quantification of the identified compounds following MS detection. Using the chromatographic conditions described above, the polyphenols all eluted in less than  $35 \text{ min}$  (Tab. 1). Four polyphenols could not be quantified under the chromatographic conditions because of overlapping (caftaric acid with gentisic acid and caffeic acid with chlorogenic acid). However, all 4 compounds were selectively identified using MS detection (qualitative analysis) based on differences in their molecular mass and MS spectra. The detection limits were calculated as the minimal concentration required to produce a reproducible peak with a signal-to-noise ratio of  $>3$ . The quantitative determinations were performed using an external standard method. Calibration curves in the  $0.5\text{--}50 \text{ } \mu\text{g} \cdot \text{L}^{-1}$  range with good linearity ( $R_2 > 0.999$ ) for a 5-point plot were used to determine the concentration of the polyphenols in the plant samples.

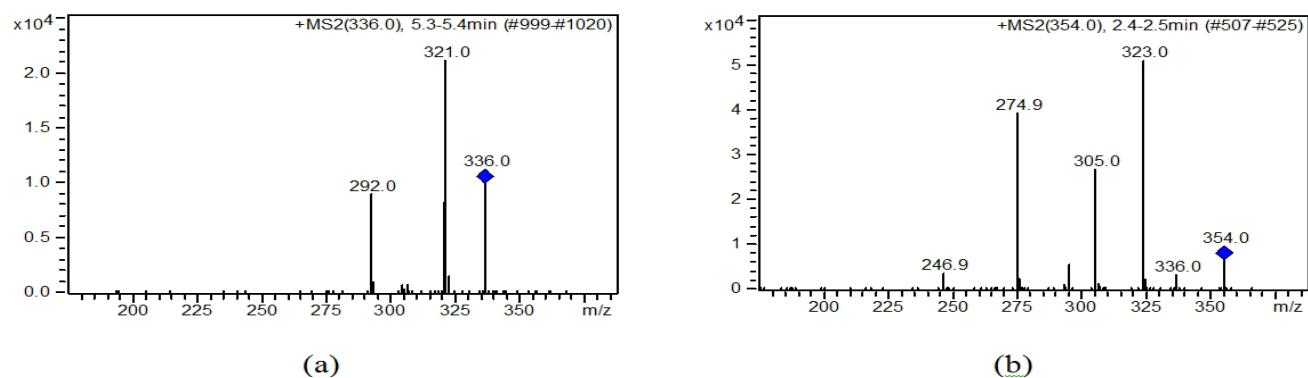


Fig. 1. ESI/MS/MS spectra of berberine (a) and chelidonium (b)

Tab. 1. Retention times (t<sub>R</sub>) for the investigated polyphenols

Peak no.	Phenolic compound	t <sub>R</sub> ± SD (min)	Peak no.	Phenolic compound	t <sub>R</sub> ± SD (min)
1	Caftaric acid*	2.10 ± 0.06	11	Myricetin	20.70 ± 0.06
2	Gentisic acid*	2.15 ± 0.07	12	Fisetin	22.60 ± 0.15
3	Caffeic acid*	5.60 ± 0.04	13	Quercitrin	23.00 ± 0.13
4	Chlorogenic acid*	5.62 ± 0.05	14	Quercetol	26.80 ± 0.15
5	p-coumaric acid	8.7 ± 0.08	15	Patuletin	28.70 ± 0.12
6	Ferulic acid	12.2 ± 0.10	16	Luteolin	29.10 ± 0.19
7	Sinapic acid	14.3 ± 0.10	17	Kaempferol	31.60 ± 0.17
8	Hyperoside	18.60 ± 0.12	18	Apigenin	33.10 ± 0.15
9	Isoquercitrin	19.60 ± 0.10			
10	Rutoside	20.20 ± 0.15			

\*overlapping UV peaks, qualitative analysis performed using MS detection

#### Identification and quantitative determinations of the sterols

The LC/MS technique was also used to analyze the sterols from the *C. majus* plant extract. The method used was a previously published HPLC method with minor changes (Sanchez-Machado *et al.*, 2004; Khalaf *et al.*, 2011). Three standards were used for the quantitative analysis, namely, beta-sitosterol, stigmasterol, and cholesterol.

#### Apparatus and chromatographic conditions

The analyses were performed using an Agilent 1100 HPLC Series system equipped with a G1322A degasser, G1311A binary pump, and G1313A autosampler. For the separation, we used a reverse-phased Zorbax SB-C18 analytical column (100 mm · 3.0 mm i.d., 5 µm particles) fitted with a precolumn Zorbax SB-C18, both operated at 40 °C. The mobile phase was prepared from methanol and acetonitrile 10:90 (v/v) isocratic elution. The flow rate was 1 mL · min<sup>-1</sup> and the injection volume was 4 µL. All solvents were filtered through 0.5-mL Sartorius filters and degassed using ultrasound. MS/MS detection using multiple reaction monitoring (MRM) of specific daughter ions was used for each sterol. The HPLC was coupled with an Agilent ion trap 1100 VL mass detector, equipped with an atmospheric pressure chemical ionization (APCI) interface working in the positive ion mode. The operating conditions were: nitrogen gas, flow rate of 7 L · min<sup>-1</sup>, heater at 400 °C, ion source temperature of 250 °C, nitrogen nebuliser at 50 psi, and capillary voltage of 4000 V. All chromatographic data were processed using ChemStation software and Data Analysis from Agilent.

#### Sterols

Under our chromatographic conditions, the retention times of the 5 analyzed sterols were 3.2 min for ergosterol, 3.9 min for brassicasterol, 4.9 min for both stigmasterol and campesterol (co-elution), and 5.7 min for beta-sitosterol. The ions monitored by the MRM method were ≤379 (253.3, 295.3, and 309.3) for ergosterol, ≤381 (201.3, 203.3, 215.2, and 217.3) for brassicasterol, ≤383

(147.3, 149.3, 161.3, and 175.3) for campesterol, ≤395 (163.3, 173.2, 187.3, 199.3, and 227.2) for stigmasterol and ≤397 (160.9, 174.9, 188.9, 202.9, and 214.9) for sitosterol. The quantitative experiments were performed using an external standard method. Calibration curves in the 60–3000 ng · mL<sup>-1</sup> range with good linearity (R<sub>2</sub> > 0.99) for a 7-point plot were used to determine the concentration of the sterols in the plant samples.

#### Determination of antifungal activity

The antifungal activity of the *C. majus* extract, expressed as the MIC, was determined by the agar-dilution assay, and was compared to the antimycotic drug fluconazole (2 mg · mL<sup>-1</sup>, Krka, Novo Mesto, Slovenia) and a control (nutritive medium and 35% ethanol). The percentage of mycelial growth inhibition (P) at each concentration was calculated using the formula  $P = (C - T) \times 100 / C$ , where C is the diameter of the control colony and T is the diameter of the treated colony (Nidiry and Babu, 2005).

#### Statistical analysis

Statistical analyses were performed using the program R environment, version 2.14.1. The results for each group were expressed as mean ± standard deviation. Data were evaluated by analysis of variance (ANOVA). A P value of ≤ 0.05 was considered statistically significant. The correlation analysis was performed by the Pearson test. Measurements of physiological processes in tulip leaves treated for 2 h with different concentrations of *C. majus* extract were performed in triplicate, and the post-ANOVA Tukey HSD test was used to analyze the significance of differences between treatments and control.

#### In vivo effect of *C. majus* extract against *B. tulipae*

Fresh tulip leaves from the field that were infected by *B. tulipae* were sprayed with the plant extract of *C. majus* at the MIC (6 %) and compared to the control tulips leaves after 2 h.

The samples of the treated leaves and control leaves were examined by transmission electron microscopy (TEM) with a JEOL JEM 1010 electron microscope (Japan Electron Optics Laboratory Co., Tokyo, Japan). Conidia controls of *B. tulipae* isolated from the tulip leaf surface were examined by scanning electron microscopy (SEM) with a JEOL JSM 5510 LV electron microscope (Hayat, 2000).

#### Measurement of leaf gas exchange

Specific gas exchange parameters were measured using a Ciras-2 leaf gas-exchange system (PP Systems) and a PLC6 automatic leaf cuvette. The photon flux density was set to  $500 \mu\text{M} \cdot \text{m}^{-2} \cdot \text{s}^{-1}$ , the air temperature in the leaf cuvette was  $26^\circ\text{C}$ , the reference carbon dioxide concentration was 340 ppm, and the reference relative air humidity was 75%. Measurements of transpiration rate, net carbon dioxide uptake, and stomatal conductivity were performed at midday, on the fully expanded leaves of the tulip (*Tulipa gesneriana* cv. 'Rococo'). Three leaves from each plant were examined at 2 h after different concentrations ofcelandine extracts were sprayed in a thin continuous layer on the leaves. The leaves were maintained for the 2 h under constant environmental conditions created in a vegetation chamber (Pinheiro et al., 2008).

#### Measurement of induced chlorophyll fluorescence parameters

The parameters of the induced chlorophyll *a* fluorescence were measured using a pulse amplitude modulated chlorophyll fluorometer (PAM-FMS2, Hansatech), on 3 leaves of each plant. The leaves were left in the dark for 10 min prior to the measurements to terminate all previous photochemical reactions. The modulated light was suffi-

ciently weak ( $0.04 \mu\text{M} \cdot \text{m}^{-2} \cdot \text{s}^{-1}$ ) so as not to produce any significant variable fluorescence. A single saturating flash ( $2,000 \mu\text{mol} \cdot \text{m}^{-2} \cdot \text{s}^{-1}$  for 0.5 s) was applied to reach the maximal fluorescence  $F_m$ . After the decline of the signal, the actinic light was turned on ( $100 \mu\text{mol} \cdot \text{m}^{-2} \cdot \text{s}^{-1}$ ) to induce the kinetics. The determined parameters were the initial fluorescence ( $F_0$ ), the maximal fluorescence ( $F_m$ ), the  $F_v/F_m$  ratio ( $F_v$  or variable fluorescence, which is the difference between the maximal and initial fluorescence), the modulated maximal fluorescence ( $F_m'$ ), the steady state fluorescence ( $F_s$ ), the effective quantum use efficiency ( $\Phi$ ) representing the ratio  $(F_m' - F_s)/F_m'$ , as well as the vitality index (relative fluorescence decrease, Rfd) expressed as the ratio  $(F_m - F_s)/F_s$  (Baker, 2008; Bartha and Fodorpataki, 2007; Horvath et al., 1996). The experimental conditions were identical to those for the leaf gas exchange measurements, and the same leaves were used for the determination of the gas exchange parameters.

## Results

The chelidonine and berberine alkaloids, polyphenols, and sterols present in the *C. majus* plant extract were determined.

The chromatograms of chelidonine (Fig. 2) and berberine (Fig. 3) from the *C. majus* extract revealed the following levels:  $26.09 \mu\text{g} \cdot \text{mL}^{-1}$  as berberine base or  $31.65 \mu\text{g} \cdot \text{mL}^{-1}$  as berberine  $\cdot \text{HCl} \cdot 2\text{H}_2\text{O}$ , and  $304.62 \mu\text{g} \cdot \text{mL}^{-1}$  as chelidonine base. The retention time for chelidonine was 2.4 min and 5.3 min for berberine.

The non-hydrolyzed sample (Fig. 4) contains rutoside ( $31.8 \mu\text{g} \cdot \text{mL}^{-1}$ ), whereas the hydrolyzed sample was determined to contain: p-coumaric acid ( $4.05 \mu\text{g} \cdot \text{mL}^{-1}$ ), ferulic

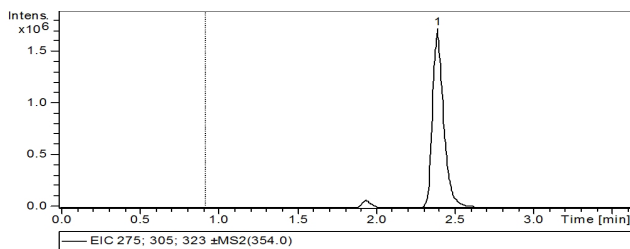


Fig. 2. Chromatogram of chelidonine from the *Chelidonium majus* extract. The chelidonine peak is marked "1"

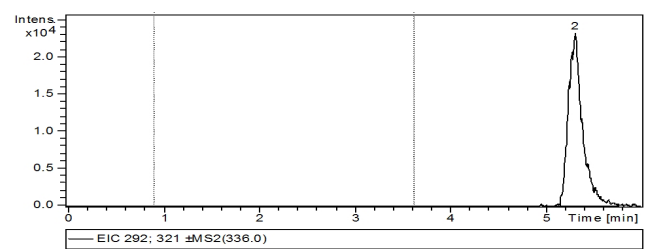


Fig. 3. Chromatogram of berberine from the *Chelidonium majus* extract. The berberine peak is marked "2"

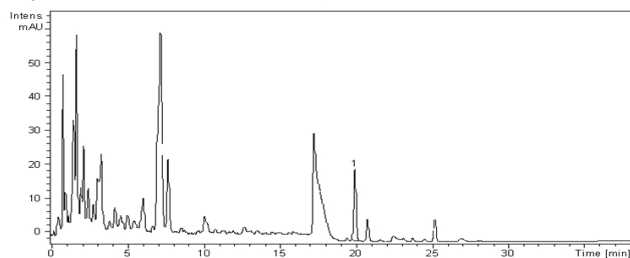


Fig. 4. Chromatogram of polyphenol rutoside from non-hydrolyzed sample of *Chelidonium majus* extract. The rutoside peak is marked "1"

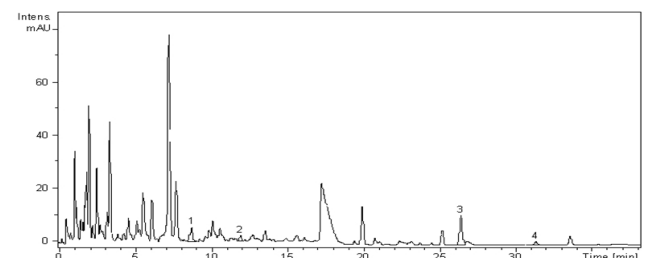


Fig. 5. Chromatogram of polyphenols from hydrolyzed sample of *Chelidonium majus* extract. The peaks are marked: "1" p-coumaric acid; "2" ferulic acid; "3" quercetol; "4" kaempferol

Tab. 2. *In vitro* effects of the *Chelidonium majus* extract on mycelial growth of *Botrytis tulipae* compared with the effects of the synthetic fungicide fluconazole

<i>Chelidonium majus</i> extract conc. (%)	<i>Botrytis tulipae</i> <sup>a</sup> Colony diameter (mm)	P <sup>b</sup> (%)	Fluconazole conc. (%)	<i>Botrytis tulipae</i> <sup>c</sup> Colony diameter (mm)	P <sup>d</sup> (%)
C	62	0	C	62	0
1	60	3.22 ± 0.23	2	44	29.03 ± 0.23
2	46	25.80 ± 0.15	4	32	48.38 ± 0.15
3	30	51.61 ± 0.15	6	21	66.12 ± 0.10
4	15	75.80 ± 0.15	8	12	80.64 ± 0.15
5	3	95.16 ± 0.16	10	4	93.54 ± 0.15
6	0	100 ± 0.21	12	0	100 ± 0.17

<sup>a</sup>Mycelial growth of *B. tulipae* at 5 days after inoculation in the presence of *C. majus*; <sup>b</sup>Inhibition % of radial growth in the presence of *C. majus*; <sup>c</sup>Mycelial growth of *B. tulipae* at 5 days after inoculation in the presence of fluconazole; <sup>d</sup>Inhibition % of radial growth in the presence of fluconazole;

C, 35% aq. EtOH;

Colony diameter is expressed as mean ± SE of 6 replicates

acid ( $0.81 \cdot \mu\text{gmL}^{-1}$ ), quercetol ( $7.88 \mu\text{g} \cdot \text{mL}^{-1}$ ), and kaempferol ( $1.21 \mu\text{g} \cdot \text{mL}^{-1}$ ) (Fig. 5).

The analyzed sample of *C. majus* extract contains stigmasterol ( $0.225 \mu\text{g} \cdot \text{mL}^{-1}$ ) and beta-sitosterol ( $0.191 \mu\text{g} \cdot \text{mL}^{-1}$ ).

The *C. majus* plant extract had a significant inhibitory effect on the mycelial growth of *B. tulipae* on culture medium. The *C. majus* MIC is 6% and the Fluconazole MIC is 12% (Tab. 2).

The *B. tulipae* control conidia were observed by electron microscopy. The SEM micrographs of the *B. tulipae* control revealed unicellular conidia with numerous randomly positioned protuberances (Fig. 6a). At the ultrastructural level, the *B. tulipae* control conidia contained a regular cell wall with a 2-layer structure, plasma membrane, cytoplasmic matrix with nucleus, and various cellular organelles, and lipids. The external cell wall layer was thin and electron dense, whereas the inner wall was thick, uniform, and less electron dense. The plasma membrane was tightly adhered to the cell wall. The cytoplasmic matrix (cytosol) was uniformly distributed, and the nucleus was  $\leq 2 \mu\text{m}$  in diameter and ovoid or spherical (Fig. 6b)

The *B. tulipae* control hyphae were observed in the attacked tulip leaf below the cuticle (Fig. 7a), in the leaf mesophyll, and near the xylem vessel (Fig. 7b). At the ultrastructural level, *B. tulipae* appears to have septate hyphae with regular cell walls and plasma membranes, as well as cytoplasmic matrices with nuclei, mitochondria, endoplasmic reticulum, lipid bodies, and glycogen (Figs. 8a and b). The parasitic activity of *B. tulipae* destroyed the attacked leaf tissues (Figs. 9a and b).

When treated with *C. majus* plant extract at the MIC for 2 h, *B. tulipae* hyphae appeared damaged at the cellular level. Specifically, the organelles were partly and/or entirely destroyed, the cytoplasm was degenerated, and electron dense material appeared in the hyphal cells. In addition, the outside of the cell wall had an irregular shape and the plasma membrane was mostly destroyed and did not adhere to the cell wall. Furthermore, precipitation of the entire cytoplasm and destroyed organelles and nuclei were seen. Because of these effects, the morpho-functional relationship between the cell wall and cytoplasm was damaged and a less electron dense band was formed between the altered cytoplasm and cell wall (Figs. 9a and b).

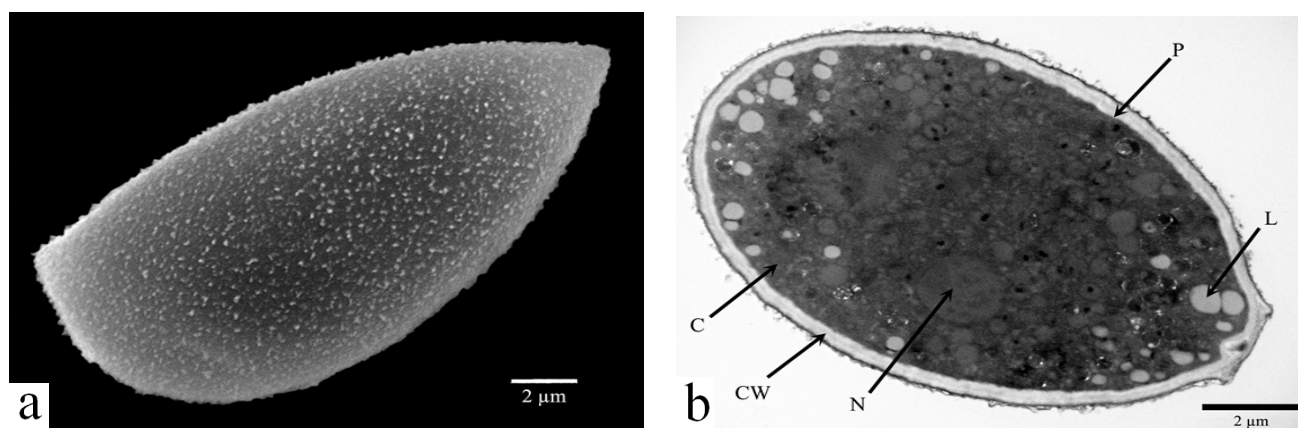


Fig. 6. Visualization of *Botrytis tulipae* conidium

a. Scanning electron micrograph showing protuberances on surface of cell wall. b. Transmission electron micrograph of an oblique section showing cell ultrastructure. CW cell wall; C cytoplasm; L lipids; N nucleus; P plasma membrane

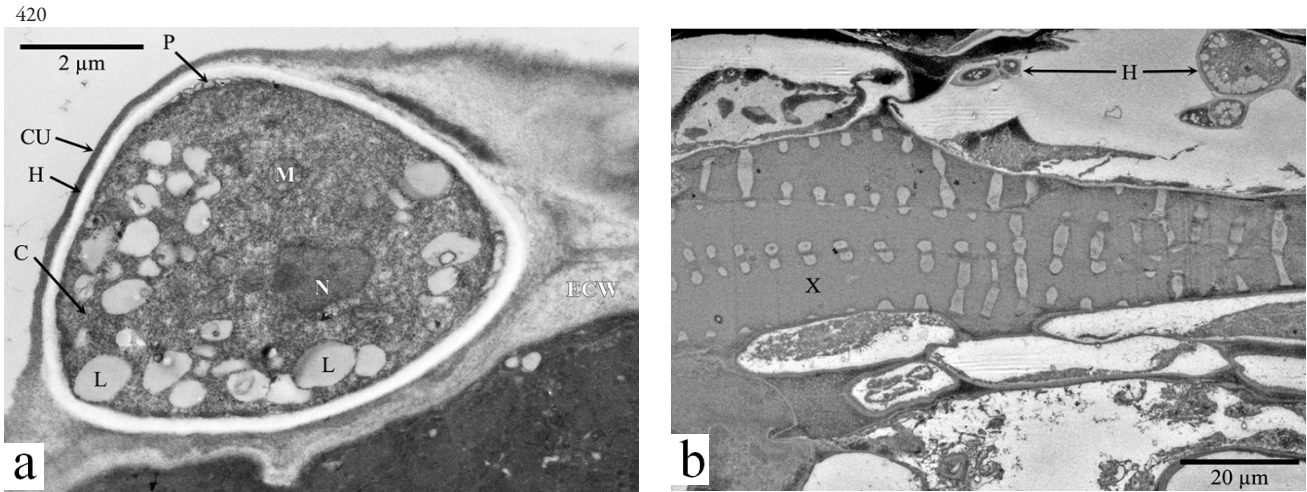


Fig. 7. Transmission electron micrograph of a tulip leaf cross section showing the *Botrytis tulipae* fungus  
 a. Hyphae (H) between the epidermal cell wall (ECW) and cuticle (CU) of the epidermis. b. Hyphae (H) in the leaf mesophyll, near the xylem (X). C cytoplasm; L lipids; M mitochondrion; N nucleus; P plasma membrane

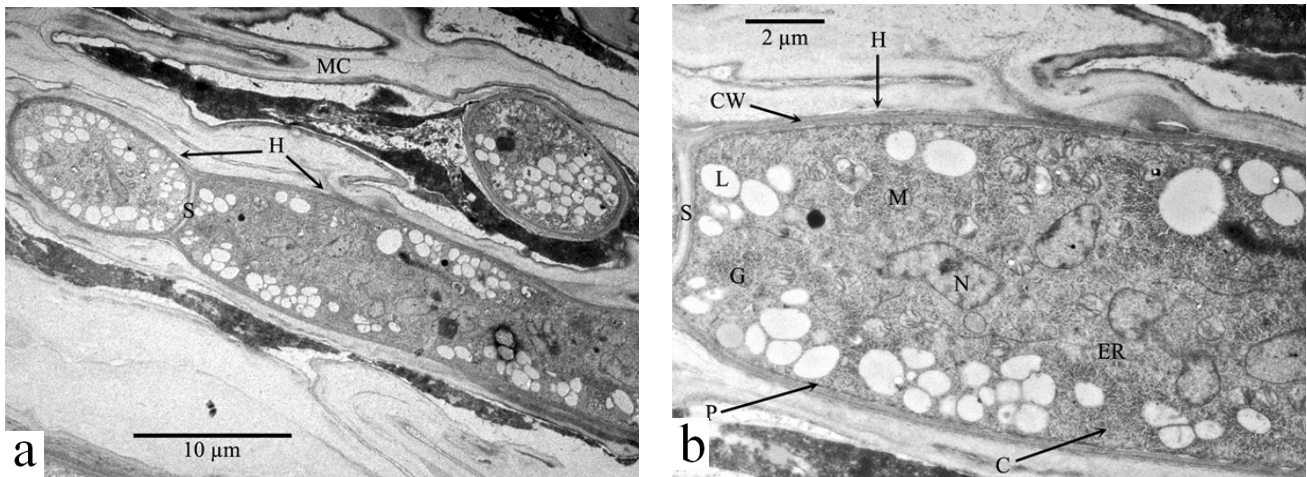


Fig. 8. Transmission electron micrograph of an oblique section of *Botrytis tulipae* control hyphae from the tulip leaf  
 a. Septate hyphae (H) in the mesophyll cells (MC). b. Detailed micrograph of septate hyphae (H) in the mesophyll. C cytoplasm; CW cell wall; ER endoplasmic reticulum; G glycogen; L lipids; M mitochondrion; N nucleus; P plasma membrane; S septum

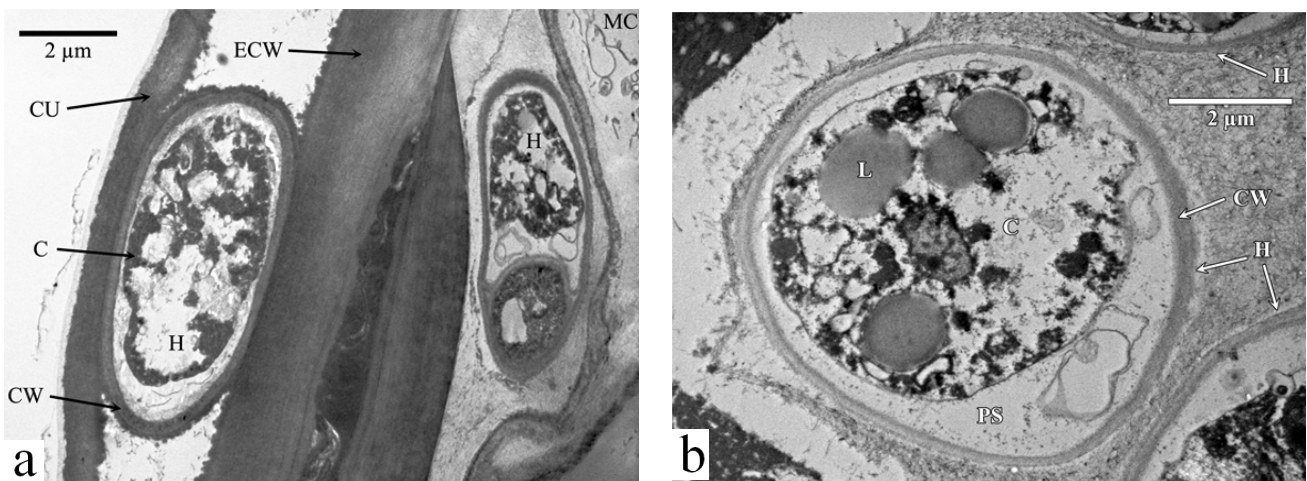


Fig. 9. Transmission electron micrograph of a tulip leaf cross section showing irreversible ultrastructural changes in *Botrytis tulipae* hyphae treated with *Chelidonium majus* plant extract at the MIC  
 a. Hyphae between the epidermal cell wall (ECW) and cuticle (CU) of the epidermis and hyphae (H) in the mesophyll cells (MC). b. hyphae (H) in the mesophyll cells (MC). C cytoplasm; CW cell wall; L lipids; PS. periplasmic space

The ground chlorophyll fluorescence was not significantly affected when the tulip leaves were covered for 2 h with solutions of 2%, 6%, and 10% extracts of celandine (Fig. 10).

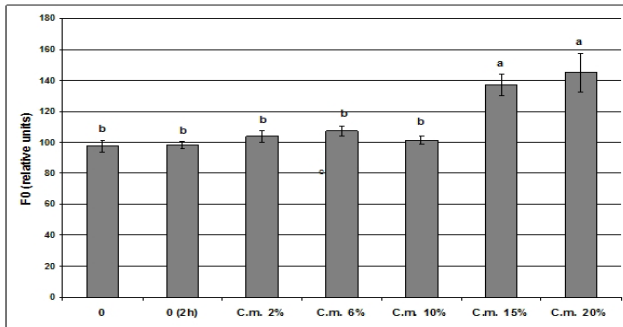


Fig. 10. Ground chlorophyll fluorescence ( $F_0$ ) in the dark-adapted tulip leaves treated for 2 h with different concentrations of celandine (C.m.) extract

0, control leaves; 0 (2 h), control leaves after 2 h. Bars represent the standard error obtained from 3 independent experiments. The letters indicate significant differences at  $p \leq 0.05$  according to the Tukey HSD test

The maximal chlorophyll fluorescence is more sensitive than the ground fluorescence, and its values were increased in the presence of 2% and 6% extracts, and decreased by 10%, 15%, and 20% celandine extracts (Fig. 11).

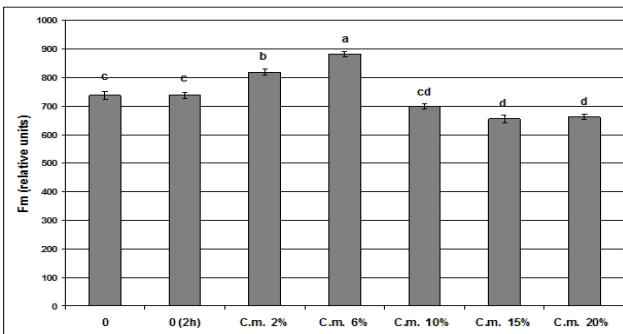


Fig. 11. Maximal chlorophyll fluorescence ( $F_m$ ) in the dark-adapted tulip leaves treated for 2 h with different concentrations of celandine (C.m.) extract

0, control leaves; 0 (2 h), control leaves after 2 h. Bars represent the standard error obtained from 3 independent experiments. The letters indicate significant differences at  $p \leq 0.05$  according to the Tukey HSD test

The potential quantum yield efficiency of photosystem II was not affected by the extract when it was sprayed on the tulip leaves at concentrations  $\leq 15\%$  (Fig. 12).

The vitality index of the photosynthetic apparatus starts to decrease significantly when the extract concentration is  $\geq 10\%$  (Fig. 13).

Progressive and statistically significant increases in all 3 gas exchange parameters (transpiration rate, net carbon dioxide uptake, and stomatal conductivity) were registered following treatment of the tulip leaves with concentrations of celandine extracts of  $\geq 6\%$  for 2 h. When the extract was used at concentrations of 2% no significant ef-

fects were noted on the investigated gas exchange parameters (Figs. 14-16).

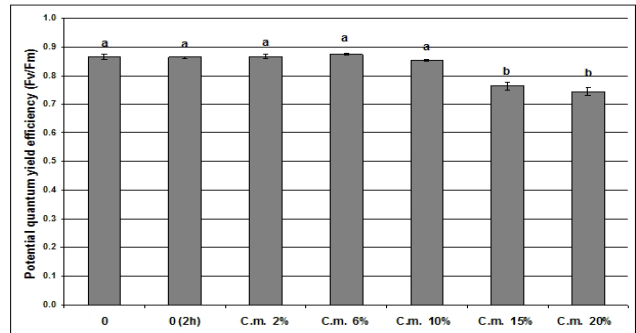


Fig. 12. Potential quantum yield efficiency of photosystem II

Values are based on the ratio between the variable and maximal chlorophyll fluorescence ( $F_v/F_m$ ) in the dark-adapted tulip leaves treated for 2 h with different concentrations of celandine (C.m.) extracts. 0, control leaves; 0 (2 h), control leaves after 2 h. Bars represent the standard error obtained from 3 independent experiments. The letters indicate significant differences at  $p \leq 0.05$  according to the Tukey HSD test

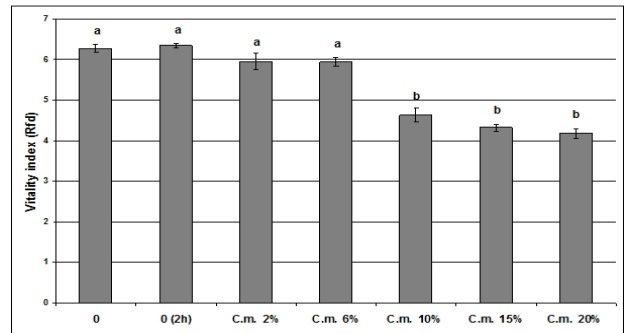


Fig. 13. Vitality index of the photosynthetic apparatus

Values are based on the relative chlorophyll fluorescence decrease ( $R_{fd}$ ) in the tulip leaves treated for 2 h with different concentrations of celandine (C.m.) extracts. 0, control leaves; 0 (2 h), control leaves after 2 h. Bars represent the standard error obtained from 3 independent experiments. The letters indicate significant differences at  $p \leq 0.05$  according to the Tukey HSD test

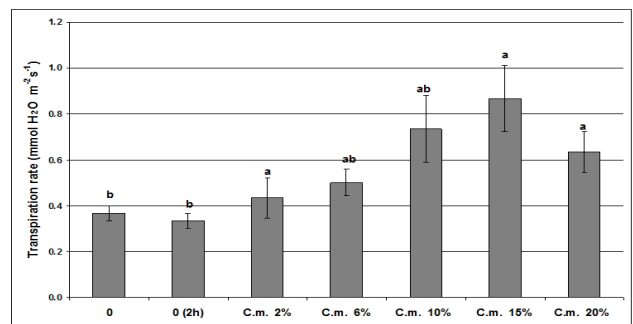


Fig. 14. Transpiration rate of the tulip leaves treated for 2 h with different concentrations of celandine (C.m.) extract

0, control leaves; 0 (2 h), control leaves after 2 h. Bars represent the standard error obtained from 3 independent experiments. The letters indicate significant differences at  $p \leq 0.05$  according to the Tukey HSD test



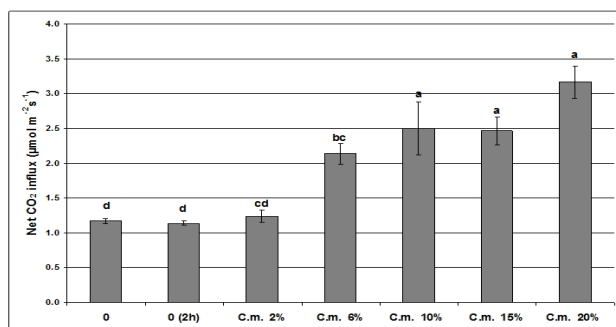


Fig. 15. Net carbon dioxide uptake by tulip leaves treated for 2 h with different concentrations of celandine (C.m.) extract

0, control leaves; 0 (2 h), control leaves after 2 h. Bars represent the standard error obtained from 3 independent experiments. The letters indicate significant differences at  $p \leq 0.05$  according to the Tukey HSD test

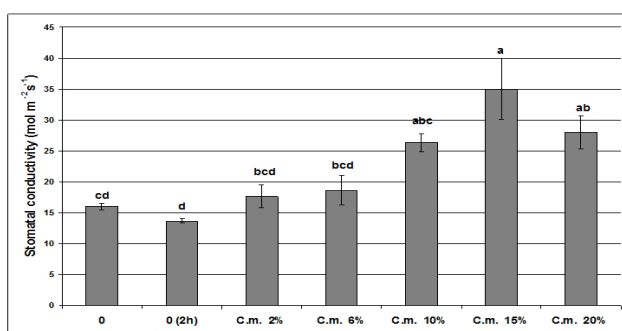


Fig. 16. Stomatal conductivity of the tulip leaves treated for 2 h with different concentrations of celandine (C.m.) extract

0, control leaves; 0 (2 h), control leaves after 2 h. Bars represent the standard error obtained from 3 independent experiments. The letters indicate significant differences at  $p \leq 0.05$  according to the Tukey HSD test

## Discussion

*B. tulipae* is the only *Botrytis* species able to infect tulip (Staats *et al.*, 2005) and to abundantly produce sporulating gray mycelium on infected tissue (Yohalem *et al.*, 2003). The mitotically produced spores, macroconidia, can be transported long distances by wind (Agrios, 2005; Webster and Weber, 2007). This parasitic fungus overwinters in the soil as mycelium in decaying plant debris and as sclerotia, which are melanized mycelial survival structures (Agrios, 2005; Yohalem *et al.*, 2003).

The *B. tulipae* conidia are ellipsoidal or obovoid, unicellular (Hong *et al.*, 2002) and have numerous randomly positioned protuberances (Fig. 6a); however, these protuberances are fewer than those present in *B. cinerea* conidia (Pârvu *et al.*, 2008). Hydration and redrying causes these protuberances to disappear (Doss *et al.*, 1997). The cell wall of the conidia has 2 layers and appears dark (Fig. 6b) because of melanin, which protects the spores from enzyme action and probably UV radiation (Epton and Richmond, 1980).

*B. tulipae* fungus penetrates tulip leaves and produces irreversible ultrastructural changes in epidermal and mes-

ophyll cells (Figs. 7 and 8). The ultrastructure of xylem cells (Fig. 7b) is not affected by the fungus and the fungus hyphae appear only in the leaf mesophyll tissues.

The infection of host plants by *B. tulipae* is mediated by numerous extracellular enzymes and metabolites. Each of these compounds plays a role in different stages of the infection process. Cutinases, lipases, and some cell wall-degrading enzymes facilitate penetration of the host surface, whereas toxins, oxalate, and reactive oxygen species enable host cell death. Several cell wall-degrading enzymes contribute to the conversion of host tissue into fungal biomass, and other enzymes such as laccases and proteases are involved in pathogenesis (Kars and van Kan, 2007).

Fungicide-resistant *Botrytis* strains have been identified in various crops (Agrios, 2005). In addition, plant fungicides based on synthetic chemicals are both pollutants and toxic (Barker and Rogers, 2006; Carrillo-Munoz *et al.*, 2006; Fatehi *et al.*, 2005; Strange and Scott, 2005; Ienaşcu *et al.*, 2008). Therefore, the biological control of *Botrytis* fungi with plant extracts is one of the important measures for enhancing farming techniques.

An important objective of our study was to test the *in vitro* action of *C. majus* extract on mycelium growth of *B. tulipae* and determine the MIC of the plant extract (Tab. 2). Previous studies suggested that *C. majus* possesses antifungal properties, and therefore, this extract is a promising source of active compounds against fungi such as *Fusarium* spp. (Matos *et al.*, 1999), *B. cinerea* (Pârvu *et al.*, 2008), and *Candida* species (Meng *et al.*, 2009).

Our study examined leaves attacked by gray mold and treated with *C. majus* extract at the MIC to demonstrate the *in vivo* inhibitory properties of the extract against *B. tulipae* (Fig. 9). The *C. majus* plant extract caused irreversible ultrastructural changes that abolished the cell wall's barrier function and its ability to activate cell wall-bound enzymes. The morpho-functional integrity of fungal cell components is required for viability and germination capacity (Isaac, 1992). The *B. tulipae* hyphae treated with *C. majus* extract revealed precipitation of the cytoplasm and destruction of organelles and nuclei that caused loss of viability and germination capacity.

In addition to the ultrastructural changes observed in *B. tulipae* hyphae treated with the plant extract (Fig. 9), the antimicrobial compounds from the *C. majus* extract induced important changes at the molecular level. The *C. majus* extract contains a large number of alkaloids and polyphenols, and is therefore, known for its antimicrobial activity (Meng *et al.*, 2009; Nawrot *et al.*, 2007; Zuo *et al.*, 2011). The main alkaloids identified in *C. majus* extracts are chelidonine, chelerythrine, sanguinarine, coptisine, and berberine (Sárközi *et al.*, 2006a; Zuo *et al.*, 2011). Formaldehyde formation due to demethylation is responsible for the antimicrobial activity of these alkaloids (Sárközi *et al.*, 2006b).

The alkaloids berberine, chelidonine, chelerythrine, sanguinarine, and coptisine (Wink, 1998) from the *C.*

*majus* plant extract induce changes at the molecular level in *B. tulipae* hyphae. Specifically, alterations involve disturbed DNA/RNA and related enzymes, as well as alterations to the cytoskeleton, ribosomal protein biosynthesis, and membrane permeability (Wink, 1998; Wink, 2008; Rosenkranz and Wink, 2008). The alkaloid berberine is present in *C. majus* extracts and *Berberis* extracts (Sárközi et al., 2006a; Zuo et al., 2011). Berberine inhibits esterases, DNA and RNA polymerases, cellular respiration, and acts in DNA intercalation (Aniszewski, 2007).

The alkaloids from *C. majus* are poisonous to *B. tulipae* fungus because they inhibit processes like DNA replication and RNA transcription that are vital for the microorganism (Wink, 1998).

Other antifungal compounds identified in the *C. majus* extract were the phenolic compounds rutoside, p-coumaric acid, ferulic acid, quercetol, and kaempherol (Tab.1). The mechanisms of action thought to be responsible for phenolic toxicity involve enzyme inhibition by the oxidized compounds, possibly through reaction with sulfhydryl groups or nonspecific interactions with the proteins (Arif et al., 2009). In addition, antifungal phenolics from plants with action against phytopathogenic fungi *B. cinerea*, *Cercospora beticola*, *Colletotrichum circinans*, *Cladosporium herbarum*, *Fusarium oxysporum*, *Phytophthora infestans*, *Venturia inaequalis*, *Verticillium albo-atrum* have been identified (Lattanzio et al., 2006).

The other antimicrobial compounds identified in the *C. majus* extract were the sterols stigmasterol ( $0.225 \mu\text{g} \cdot \text{mL}^{-1}$ ) and beta-sitosterol ( $0.191 \mu\text{g} \cdot \text{mL}^{-1}$ ). The most abundant plant sterols are sitosterol, campesterol, and stigmasterol (Moreau et al., 2002), and the antifungal activity of plant sterols (Sharma and Kumar, 2009) and sterols from *Ganoderma annulare* mushroom have been described (Smania et al., 2003). Moreover, free flavonoids and sterols of the *Tridax procumbens* plant extract completely inhibited spore germination of the *F. oxysporum* phytopathogenic fungus (Sharma and Kumar, 2009).

Our results reveal that the *C. majus* extract contains important antifungal compounds like alkaloids, phenols, and sterols. Importantly, these results clarify the antifungal activity of *C. majus* against phytopathogenic fungi (Matos et al., 1999; Pârnu et al., 2008) such as *B. tulipae*. The *C. majus* extract at MIC (6%) caused irreversible changes in *B. tulipae* hyphae, and therefore, *in vivo* studies examining the effect of the extract on tulips that have not been attacked by gray mold is required.

Whenever environmental stress factors directly or indirectly influence the energetic processes that occur during photosynthesis, they cause specific changes in the various parameters associated with induced chlorophyll fluorescence (Baker and Oxborough, 2004). This enables a quick *in situ* evaluation of alterations to photosynthesis in tulip leaves treated with antifungal celandine extracts. This is important because any agent used in pest management

must be effective against parasites and minimally affect the vital processes of the host plant. *In vivo* induced chlorophyll fluorescence is a sensitive, non-destructive tool for the study of environmental impacts on the primary energy-conversion processes of photosynthesis. The potential quantum use efficiency of photosynthesis is reflected by the ratio between the variable and the temporary maximal fluorescence yield ( $F_v/F_m$ ) in dark-adapted leaves. The  $F_v/F_m$  value is one of the most relevant functional markers of photosynthetic energy conversion, and therefore is used for detection of various stress factors that interfere with photochemical reactions in chloroplasts. Its drop below the value of 0.8 is directly related to the disturbed photochemical reactions that occur in photosystem II of thylakoid membranes in chloroplast, which leads to a less efficient photosynthetic use of the absorbed light energy. The initial fluorescence of the dark-adapted leaves ( $F_0$ ), which is induced by a very weak red light flash, is related to the organization and energy transfer capacity of the light-harvesting antennae. The maximal fluorescence ( $F_m$ ), which is generated by a flash of saturating red light, is related to the activity of the electron acceptors of photosystem II. One of the most sensitive parameters of induced chlorophyll fluorescence is the relative fluorescence decrease ( $R_{fd}$ ), which is also known as the vitality index. This value is dependent on the difference between the temporary maximal fluorescence yield in dark-adapted samples and the steady state fluorescence level in constantly illuminated samples. The pulse amplitude modulation of chlorophyll fluorescence is obtained by regular saturating flashes on a background of a constant actinic light (Baker, 2008).

Because the ground chlorophyll fluorescence of the dark-adapted leaves was not significantly affected, one can deduce that the organization and energy transfer function of the light-harvesting pigment antennae of the leaves were not impaired by extract concentrations  $\leq 15\%$ . The registered values of maximal chlorophyll fluorescence indicate that small amounts of the celandine extract slightly stimulate photochemical reactions on the acceptor side of photosystem II (e.g., reduction of quinone acceptors), whereas higher extract concentrations moderately inhibit them, without causing a dramatic decline in the process. The fact that potential quantum yield efficiency of photosystem II was not affected by the extract implies that the overall conversion of light energy into storable chemical energy is not altered when plants are treated with dilute extracts of celandine. This is also valid for the vitality index of the photosynthetic apparatus, which is more sensitive than quantum efficiency, and decreases only upon treatment with extract concentrations reaching or exceeding 10% (Figs. 10-13). Based on the parameters of induced chlorophyll fluorescence, one can state that the photosynthetic light conversion capacity of tulip leaves is not reduced by the application of celandine extracts at concentrations of 2% or 6%.

Gas exchange processes through the leaf surfaces may be directly influenced by any substance that is sprayed onto the leaves, and may thus, penetrate the cuticle or enter the leaf through open stomata. This can lead to disturbances in carbon dioxide supply for photosynthetic carbon assimilation, or to an impaired regulation of stomatal movements that can threaten the water equilibrium and inorganic nutrient uptake of the whole plant. Therefore, it is important to investigate the effect of depositing celandine extracts on leaves on gas exchange processes. In the water economy of plants, the most important gas exchange parameter is transpiration rate, whereas for the photosynthetic carbon assimilation, net carbon dioxide uptake is a crucial prerequisite. The overall dynamics of gas exchange on the leaf surface is indicated by stomatal conductivity. For example, the intensity of the gas exchange processes per unit leaf area strongly decreases during drought and salt stress, as well as under the influence of different air pollutants (Allen and Percy, 2000; Medrano *et al.*, 2002; Hetherington and Woodward, 2003).

The results of the gas exchange measurements suggest that if the celandine extract is sprayed on tulip leaves at concentrations higher than 2%, it may cause increased transpirational water loss, which may also be beneficial if excess water is present in the soil and the higher suction force enhances the uptake of inorganic nutrients from the soil, and may ensure a better carbon dioxide supply to the leaves through the more widely open stomata. No inhibition of gas exchange processes were detected even when the celandine extract was applied at higher concentrations.

### Conclusions

The *C. majus* plant extract exhibited strong *in vitro* and *in vivo* fungicidal activity against *B. tulipae*. The *C. majus* plant extract at the MIC caused severe ultrastructural changes in the tulip leaf hyphae that lead to loss of viability. The *Botrytis* strains have a high resistance to conventional fungicides, and therefore, we propose that *C. majus* is a good *in vivo* biological treatment against fungal infections like gray mold (Parvu *et al.*, 2008), tulip mold, and other species (Matos *et al.*, 1999). After 2 h of surface treatment under growth chamber conditions, low concentrations (2%) of celandine extract did not affect the main physiological parameters associated with leaf gas exchange and photosynthetic light-use efficiency. The transpiration rate, net carbon dioxide influx, and overall stomatal conductivity increased at concentrations greater than 6%, thereby indicating stimulated stomatal opening, which favors carbon assimilation but may impair water economy. The ground fluorescence of chlorophyll *a* indicated that light harvesting by photosynthetic antenna pigments was affected only by higher concentrations (15% and 20%) of celandine extract. The maximal chlorophyll fluorescence yield of dark-adapted leaves, which is related to the photochemical processes on the acceptor side of photosystem

II, increased upon treatment with lower concentrations (2% and 6%) of extract, but declined when the leaves were sprayed with higher concentrations (10-20%). The main efficiency parameters of photosynthesis, such as potential quantum yield efficiency and overall vitality index, were not affected by the extract when its concentration was  $\leq 10\%$ .

In conclusion, we recommend the use of the celandine extract in concentration of 6% for the efficient protection of tulips against the attack of gray mold.

### Acknowledgment

These studies were financially supported by the Romanian Ministry of Education and Research from the CNC-SIS grants 46/220/2006, 43/220/2007, and PNII-IDEI 2272/2009-2011.

### References

- Agrios GN (2005). Plant Pathology 5<sup>th</sup> ed. Elsevier, Amsterdam, 510 p.
- Allen MT, Percy RW (2000). Stomatal behavior and photosynthetic performance under dynamic light regimes in a seasonally dry tropical rain forest. *Oecologia* 122:470-478.
- Aniszewski T (2007). Alkaloids-secrets of Life Alkaloid Chemistry, Biological Significance, Applications and Ecological Role. Elsevier, Amsterdam, 181 p.
- Arif T, Bhosale JD, Kumar N, Mandal TK, Bendre RS, Lavekar GS, Dabur R (2009). Natural products – antifungal agents derived from plants. *J Asian Nat Prod Res* 11:621-638.
- Arif T, Mandal TK, Dabur R (2011). Natural products: Antifungal agents derived from plants, p. 283-311. In: Tiwari VK (Ed.). Opportunity, Challenge and Scope of Natural Products in Medicinal Chemistry. Research Signpost, Kerala (India).
- Baker NR (2008). Chlorophyll fluorescence: a probe of photosynthesis *in vivo*. *Annu Rev Plant Biol* 59:89-113.
- Baker NR, Oxborough K (2004). Chlorophyll fluorescence as a probe of photosynthetic productivity, p. 65-82. In: Papageorgiou GC, Govindjee (Eds.). Chlorophyll *a* Fluorescence: A Signature of Photosynthesis. Springer, Dordrecht.
- Barker KS, Rogers PD (2006). Recent insights into the mechanisms of antifungal resistance. *Curr Infect Dis Rep* 8:449-456.
- Bartha L, Fodorpataki L (2007). Physiological reactions of the succulent CAM plant *Bryophyllum daigremontianum* to increased salinity. *Contrib Bot* 42:47-56.
- Beever RE, Weeds PL (2007). Taxonomy and genetic variation of *Botrytis* and *Botryotinia*, p. 29-52. In: Elad Y, Williamson B, Tudzynski P, Delen N (Eds.). *Botrytis*: Biology, Pathology and Control. Springer, Dordrecht.
- Carrillo-Munoz AJ, Giusiano G, Ezkurra PA, Quindos G (2006). Antifungal agents: mode of action in yeast cells. *Rev Esp Quimioter* 19:130-139.

- Choi GJ, Jang KS, Kim JS, Lee SW, Cho JY, Cho KY, Kim JC (2004). *In vivo* antifungal activities of 57 plant extracts against six plant pathogenic fungi. *Plant Pathol J* 20:184-191.
- Compaore M, Lamien CE, Lamien-Meda A, Vlase L, Kien-drebeogo M, Ionescu C, Nacoulma OG (2012). Antioxidant, xanthine oxidase and lipoxygenase inhibitory activities and phenolics of *Bauhinia rufescens* Lam. (Caesalpinaceae). *Nat Prod Res* 26:1069-1074.
- Doss RP, Christian JK, Potter SW, Soeldner AH, Chastagner GA (1997). The conidial surface of *Botrytis cinerea* and several other *Botrytis* species. *Can J Bot* 75:612-617.
- Elad Y, Stewart A (2004). Microbial control of *Botrytis* spp., p. 223-241. In: Elad Y, Williamson B, Tudzynski P, Delen N (Eds.). *Botrytis: Biology, Pathology and Control*. Springer, Dordrecht.
- Elad Y, Williamson B, Tudzynski P, Delen N (2007). *Botrytis* spp. and diseases they cause in agricultural systems – an introduction, p. 1-8. In: Elad Y, Williamson B, Tudzynski P, Delen N (Eds.). *Botrytis: Biology, Pathology and Control*. Springer, Dordrecht.
- Epton HAS, Richmond DV (1980). Formation, structure and germination of conidia, p. 41-83. In: Coley-Smith JR, Verhoeff K, Jarvis WR (Eds.). *The Biology of Botrytis*. Academic Press, London.
- Fatehi M, Saleh TM, Fatehi-Hassanabad Z, Farrokhfal K, Davodi SJ (2005). A pharmacological study on *Berberis vulgaris* fruit extract. *J Ethnopharmacol* 102:46-52.
- Hayat MA (2000). *Principles and Techniques of Electron Microscopy: Biological Applications*. University Press, Cambridge, 1 p.
- Hetherington AM, Woodward FI (2003). The role of stomata in sensing and driving environmental change. *Nature* 424:901-908.
- Hong SK, Kim WG, Cho WD, Kim HG (2002). Occurrence of tulip fire caused by *Botrytis tulipae* in Korea. *Plant Pathol J* 18:106-108.
- Horvath G, Droppa M, Fodorpataki L, Istokovics A, Garab G, Oettmeier W (1996). Acridones: a chemically new group of protonophores. *Proc Nat Acad Sci USA* 93:3876-3880.
- Ienașcu IMC, Lupea AX, Hădăruga D, Hădăruga N, Popescu IM (2008). The antimicrobial activity and quantitative structure – biological activity relationships evaluation of some novel 2-hydroxybenzamide derivatives. *Revista de Chimie* 59:247-250.
- Isaac S (1992). *Fungal-Plant Interactions*. Chapman & Hall, London, 10 p.
- Kars I, van Kan JAL (2007). Extracellular enzymes and metabolites involved in pathogenesis of *Botrytis*, p. 99-118. In: Elad Y, Williamson B, Tudzynski P, Delen N (Eds.). *Botrytis: Biology, Pathology and Control*. Springer, Dordrecht.
- Khalaf I, Corciova A, Vlase L, Ivănescu B, Lazăr D (2011). LC/MS analysis of sterolic compounds from *Glycyrrhiza glabra*. *Studia UBB Chemia* 56:97-102.
- Lattanzio V, Lattanzio VMT, Cardinali A (2006). Role of phenolics in the resistance mechanisms of plants against fungal pathogens and insects, p. 23-67. In: Imperato F (Ed.). *Phytochemistry: Advances in Research*. Trivandrum, Kerala (India).
- Matos OC, Baeta J, Silva MJ, Pinto Ricardo CP (1999). Sensitivity of *Fusarium* strains to *Chelidonium majus* L. extracts. *J Ethnopharmacol* 66:151-168.
- Meda RNT, Vlase L, Lamien-Meda A, Lamien CE, Muntean D, Tipericiu B, Oniga I, Nacoulma OG (2011). Identification and quantification of phenolic compounds from *Balanites aegyptiaca* (L) Del (Balanitaceae) galls and leaves by HPLC-MS. *Nat Prod Res* 25:93-99.
- Medrano H, Escalona MH, Bota JM, Gulias J, Flexas J (2002). Regulation of photosynthesis of C<sub>3</sub> plants in response to progressive drought: stomatal conductance as a reference parameter. *Ann Bot* 89:895-905.
- Meng FY, Zuo GY, Hao XY, Wang GC, Xiao HT, Zhang JQ, Xu GL (2009). Antifungal activity of the benzo[c]phenanthridine alkaloids from *Chelidonium majus* Linn against resistant clinical yeast isolates. *J Ethnopharmacol* 125:494-496.
- Mishra R, Verma DL (2009). Antifungal activity and flavonoid composition of *Wiesnerella denudata*. *Steph Acad Arena* 1:42-45.
- Moreau R, Whitaker B, Hicks K (2002). Phytosterols, phytostanols, and their conjugates in foods: structural diversity, quantitative analysis, and health-promoting uses. *Prog Lipid Res* 41:457-500.
- Nawrot R, Lesniewicz K, Pienkowska J, Gozdzicka-Jozefiak A (2007). A novel extracellular peroxidase and nucleases from a milky sap of *Chelidonium majus*. *Fitoterapia* 78:496-501.
- Nencu I, Vlase L, Istudor V, Dutu LE, Gird CE (2012). Preliminary research regarding the therapeutic uses of *Urtica dioica* L. Note I. The polyphenols evaluation. *Farmacia* 60:493-500.
- Nidiry ESJ, Babu CSB (2005). Antifungal activity of tuberose absolute and some of its constituents. *Phytother Res* 19:447-449.
- Pârvu M, Pârvu AE (2011). Antifungal plant extracts, p.1055-1062. In: Méndez-Vilas A (Ed.). *Science Against Microbial Pathogens: Communicating Current Research and Technological Advances*. Formatex Research Center, Badajoz (Spain).
- Pârvu M, Pârvu AE, Crăciun C, Barbu-Tudoran L, Tămaș M (2008). Antifungal activities of *Chelidonium majus* extract on *Botrytis cinerea* *in vitro* and ultrastructural changes in its conidia. *J Phytopathol* 156:550-552.
- Pinheiro HA, Silva JV, Endres L, Ferreira VM, Camara CA, Cabral FF, Oliveira JF, Carvalho LWT, Santos JM, Filho BGS (2008). Leaf gas exchange, chloroplastic pigments and dry matter accumulation in castor bean (*Ricinus communis* L) seedlings subjected to salt stress conditions. *Ind Crop*

- Prod 27:385-392.
- Rosenkranz V, Wink M (2008). Alkaloids induce programmed cell death in bloodstream forms of trypanosomes (*Trypanosoma b. brucei*). *Molecules* 13:2462-2473.
- Sanchez-Machado DI, Lopez-Hernandez J, Paseiro-Losada P, Lopez-Cervantes J (2004). An HPLC method for the quantification of sterols in edible seaweeds. *Biomed Chromatogr* 18:183-190.
- Sárközi Á, Janicsák G, Kursinszki L, Kéry Á (2006a). Alkaloid composition of *Chelidonium majus* L. studied by different chromatographic techniques. *Chromatographia* 63:81-86.
- Sárközi Á, Móricz ÁM, Ott PG, Tyihák E, Kéry Á (2006b). Investigation of *Chelidonium* alkaloids by use of a complex bioautographic system. *J Planar Chromatogr* 19:267-272.
- Sharma B, Kumar P (2009). In vitro antifungal potency of some plant extracts against *Fusarium oxysporum*. *Int J Green Pharm* 3:63-65.
- Smania EF, Delle Monache F, Smania A, Yunes RA, Cuneo RS (2003). Antifungal activity of sterols and triterpenes isolated from *Ganoderma annulare*. *Fitoterapia* 74:375-377.
- Staats M, van Baarlen P, van Kan JA (2005). Molecular phylogeny of the plant pathogenic genus *Botrytis* and the evolution of host specificity. *Mol Biol Evol* 22:333-346.
- Staats M, van Baarlen P, van Kan JAL (2007). AFLP analysis of genetic diversity in populations of *Botrytis elliptica* and *Botrytis tulipae* from the Netherlands. *Eur J Plant Pathol* 117:219-235.
- Strange RN, Scott PR (2005). Plant disease: a threat to global food security. *Annu Rev Phytopathol* 43:83-116.
- Sundaram U, Gurumoorthi P (2012). Validation of HPTLC method for quantitative estimation of L-Dopa from *Mucuna pruriens*. *Int Res J Pharm* 3:300-304.
- Webster JW, Weber RWS (2007). *Introduction to Fungi*. University Press, Cambridge, 434 p.
- Wilson CL, Solar JM, El Ghaouth A, Wisniewski ME (1997). Rapid evaluation of plant extracts and essential oils for antifungal activity against *Botrytis cinerea*. *Plant Dis* 81:204-210.
- Wink M (1998). Modes of action of alkaloids, p. 301-326. In: Roberts MF, Wink M (Eds.). *Alkaloids: Biochemistry, Ecology, and Medicinal Applications*. Plenum Press, New York.
- Wink M (2008). Ecological roles of alkaloids, p. 3-23. In: Fattorusso E, Tagliatela-Scafati O (Eds.). *Modern Alkaloids Structure, Isolation, Synthesis and Biology*. WILEY-VCH Verlag GmbH & Co. KGaA, Weinheim.
- Wu W, Song F, Yan C, Liu Z, Liu S (2005). Structural analyses of protoberberine alkaloids in medicine herbs by using ESI-FT-ICR-MS and HPLC-ESI-MS(n). *J Pharm Biomed Anal* 37:437-46.
- Yohalem DS, Nielsen K, Nicolaisen M (2003). Taxonomic and nomenclatural clarification of the onion neck rotting *Botrytis* species. *Mycotaxon* 85:175-182.
- Zuo G-Y, Meng F-Y, Han J, Hao X-Y, Wang G-C, Zhang Y-L, Zhang Q (2011). *In vitro* activity of plant extracts and alkaloids against clinical isolates of extended-spectrum  $\beta$ -lactamase (ESBL)-producing strains. *Molecules* 16:5453-5459.